Progress In Electromagnetics Research, PIER 79, 59–74, 2008

MODAL ANALYSIS OF EXTRAORDINARY TRANSMISSION THROUGH AN ARRAY OF SUBWAVELENGTH SLITS

G. Ghazi and M. Shahabadi

Center of Excellence for Applied Electromagnetics Systems
Photonics Research Lab.
School of Electrical and Computer Engineering
University of Tehran
Tehran, Iran

Abstract—Using eigen-modes of a one-dimensional array of slits together with a mode matching technique, we investigate the extraordinary transmission through a subwavelength grating. The analysis serves to determine the contribution of various transmission mechanisms to the overall transmission. It is shown that surface plasmon polaritons excited on the input interface of the grating at certain wavelengths can absorb the incident power and thus reduce the total transmitted power. We also examine the characteristics of the different types of modes involved in the transmission through a metallic grating.

1. INTRODUCTION

Surface plasmon polariton according to Reather [4] is a localized wave on the interface of metal and dielectric for which the propagation constant along the interface can be obtained from Maxwell's equations as: $k_{sp} = k_o\sqrt{\varepsilon_{rm}\varepsilon_{rd}/(\varepsilon_{rm}+\varepsilon_{rd})}$ where ε_{rm} and ε_{rd} are the relative permittivities of metal and dielectric, respectively, and k_o is the free-space wavenumber. These waves on a metal-dielectric interface offered a new way to nanophotonics, such as refractive-index measurements [2] and enhanced light transmission in subwavelength metallic structures [3, 4]. At microwave frequencies analysis of metallic strip gratings have been done assuming that the metals are perfect electric conductors (PEC) [5, 6]. Thin wire two-dimentional gratings at these frequencies have been proposed for increasing antenna gain as a metamaterial [7, 8]. At optical wavelengths the losses in metals are important and

the complex permittivity of metals should be considered investigating such metallic gratings. According to the Bethe theory of small apertures, optical transmission through subwavelength apertures must be negligible [9]. However, in the recent decade, certain experiments have verified that an extraordinary optical transmission is possible if there is a periodic array of subwavelength holes in a thin metallic film [10]. Because of the potential applications of this effect in nano-photonic technology, there have been many theoretical and experimental investigations to explain the origin of the extraordinary transmission. The investigation of this phenomenon in one-dimensional slits smaller than half a wavelength is more complicated than in two-dimensional arrays since for the former, there exists a guided mode without cut-off. In the one-dimensional slit arrays, the mechanism of transmission is explained from different standpoints. Porto et al. using the transfer matrix method, show that it is the surface plasmon polaritons (SPP) which mainly contribute to the transmission [11]. Subsequent theoretical studies of complex band structure of transmission gratings [12] have also suggested the existence of coupled surface resonances and cavity modes. In [13], Lalanne et al. using a rigorous coupled wave analysis (RCWA), conclude that high transmission is due to diffraction and waveguide mode resonances and that SPP can reduce transmission efficiency. In his paper, Treacy has summarized three physical models for explaining high transmission and has shown that the dynamic diffraction theory can explain the transmission mechanism properly [14]. Other analytical works based on the modal expansion are presented in [15, 16] and [17] to explain the interaction of light and gratings. In [17], the excitation of the grating modes in a semi-infinite grating and the transfer of power just after interface are examined. It is concluded that the guided mode plays an important role in power transmission. Finite-difference time-domain (FDTD) method is also used for investigation of the problem. For instance, [18] shows that the high transmission occurs when the period of the structure is slightly shorter the wavelength of SPP. Here, the current present in the slits supports the guided mode and is responsible for the transmission.

In the present paper, we carry out a modal analysis for a periodic array of subwavelength slits realized in a thin silver layer. The transmission efficiency of such a grating is calculated by matching the tangential fields outside the grating to the eigen-modes inside the grating. Using this approach, we accurately describe the influence of the excitation of the guided mode as well as the SPP on the total transmission through the grating.

2. MODAL EXPANSION IN DIFFERENT REGIONS

Figure 1 shows a periodic array of slits in a metallic layer suspended in air. The array is illuminated by a plane wave propagating in region I The fields in the air regions (regions I and III) can be expressed as a Rayleigh expansion. In the grating region (region II), to obtain the eigen-modes, Maxwell's equations are solved with appropriate periodic boundary conditions. For this structure, two uncoupled TM_z (Transverse Magnetic to the z direction) and TE_z (Transverse Electric to the z direction) polarizations exist. For the TM_z polarization, there always exists a guided mode, but for the TE_z polarization when the width of the slits is less than $\lambda_o/2$, where λ_o is the free-space wavelength, all the modes are below cut-off. Since TM_z polarization shows extraordinary transmission effect in subwavelength periodic arrays, we will mainly examine this polarization, by determining the only nonzero field components (H_x, E_y, E_z).

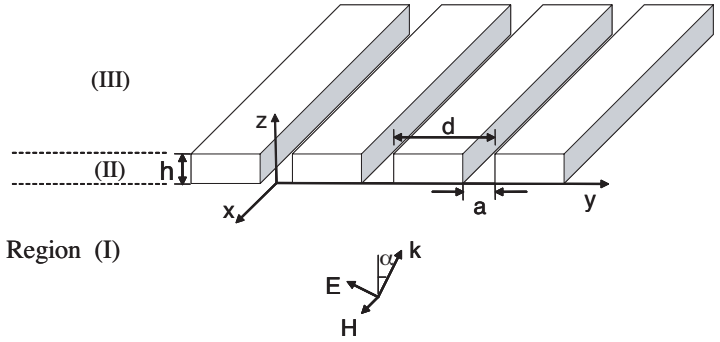

Figure 1. Grating structure excited by a plane wave.

The magnetic field for the eigen-modes of region II in Fig. 1 is expressed by

$$H_x^{(n)II} = \begin{cases} \left[A'_n \cos\left(v_n\left(y-\frac{a}{2}\right)\right) + B'_n \sin\left(v_n\left(y-\frac{a}{2}\right)\right)\right] e^{-jk_{zn}z} \\ \qquad\qquad \text{for } \frac{a}{2} \le y \le d-\frac{a}{2} \\ \left[C'_n \cos\left(u_n\left(y+\frac{a}{2}\right)\right) + D'_n \sin\left(u_n\left(y+\frac{a}{2}\right)\right)\right] e^{-jk_{zn}z} \\ \qquad\qquad \text{for } -\frac{a}{2} \le y \le \frac{a}{2} \end{cases} . \tag{1}$$

Here, n is the mode index ($n = 1, 2, 3, \ldots$) and $u_n = \sqrt{k_0^2 - k_{zn}^2}$,

$v_n = \sqrt{\varepsilon_{rm} k_0^2 - k_{zn}^2}$ where ε_{rm} is the complex permittivity of the metal at the wavelength of operation. Derivation of other field components from Maxwell's equations is straightforward. The tangential field components $(H_x^{(n)}, E_z^{(n)})$ are matched on the vertical boundary of metal and dielectric which is assumed to be air. The continuity of the tangential field components together with the Bloch condition of the periodic structure, i.e.,

$$\begin{aligned} H_x^{(n)II}\left(y = d - \frac{a}{2}\right) &= e^{-j(k_0 \sin\alpha)d} H_x^{(n)II}\left(y = -\frac{a}{2}\right), \\ E_z^{(n)II}\left(y = d - \frac{a}{2}\right) &= e^{-j(k_0 \sin\alpha)d} E_z^{(n)II}\left(y = -\frac{a}{2}\right) \end{aligned} \tag{2}$$

yields a linear system of four equations. From this system, we can obtain the matrix equation for the unknown coefficients of (1) as:

$$\begin{bmatrix} 1 & 0 & -\cos(u_n a) & -\sin(u_n a) \\ 0 & \dfrac{v_n}{\varepsilon_r} & u_n \sin(u_n a) & -u_n \cos(u_n a) \\ \cos(v_n(d-a)) & \sin(v_n(d-a)) & -e^{-j(k_0 \sin\alpha)d} & 0 \\ -\dfrac{v_n}{\varepsilon_r}\sin(v_n(d-a)) & \dfrac{v_n}{\varepsilon_r}\cos(v_n(d-a)) & 0 & -e^{-j(k_0 \sin\alpha)d} u_n \end{bmatrix} \begin{bmatrix} A'_n \\ B'_n \\ C'_n \\ D'_n \end{bmatrix} = 0. \tag{3}$$

Existence of a nontrivial solution of the system of equations requires that the determinant of the matrix be zero which results in

$$\begin{aligned} &\frac{u_n v_n}{\varepsilon_{rm}} \cos(k_0 d \sin\alpha) - \frac{u_n v_n}{\varepsilon_{rm}} \cos(u_n a)\cos(v_n(d-a)) \\ &\quad + \frac{1}{2}\left(u_n^2 + \frac{v_n^2}{\varepsilon_{rm}^2}\right)\sin(u_n a)\sin(v_n(d-a)) = 0. \end{aligned} \tag{4}$$

Equation (4) together with the relations for v_n and u_n can be solved for k_{zn}. When the incidence is normal, i.e., $\alpha = 0$, because of some symmetry, Equation (4) reduces to

$$v_n \cos\left(u_n \frac{a}{2}\right)\sin\left(v_n \frac{(d-a)}{2}\right) + u_n \varepsilon_{rm} \sin\left(u_n \frac{a}{2}\right)\cos\left(v_n \frac{(d-a)}{2}\right) = 0. \tag{5}$$

In the two homogeneous regions, the H_x components can be expressed as a summation of the Rayleigh modes, i.e.,

$$H_x^I = \sum_{m=-M}^{M} \left(A_m e^{-jk_{ym}y} e^{-j\tilde{k}_{zm}z} + B_m e^{-jk_{ym}y} e^{j\tilde{k}_{zm}z} \right), \quad (6)$$

$$H_x^{III} = \sum_{m=-M}^{M} A''_m e^{-jk_{ym}y} e^{-j\tilde{k}_{zm}z}, \quad (7)$$

where $k_{ym}^2 + \tilde{k}_{zm}^2 = k_o^2,\ k_{ym} = \dfrac{2m\pi}{d} + k_o \sin\alpha$. From these waves and Maxwell's equations, we can determine other field components. The obtained H_x and E_y field components in the three regions are then used for mode matching on the input and output interfaces of the metallic grating. Before doing so, we examine the modes inside the metallic grating region.

3. MODAL ANALYSIS IN THE METALLIC GRATING

Equation (4) or Equation (5) is solved for the complex propagation constant k_{zn}. The obtained propagation constants are normalized to k_o. Throughout this paper, we have assumed $e^{+j\omega t}$ as time dependence. Under this assumption, we choose those roots of the transcendental equation which have a negative imaginary part. We will assume the form $k_{zn} = \beta - j\alpha$, so α is positive while β can assume both positive and negative values. Fig. 2 illustrates the loci of the propagation constant k_{zn} for various modes of region II. Figs. 2(a) and (b) are plotted for two different slit widths $a/\lambda_o = 0.5$ and $a/\lambda_o = 0.1$, respectively. In these figures, as we expected for the TM_z polarization, there is at least one propagating mode, i.e., a mode with a vanishing attenuation constant. Note that as the slit width reaches half a wavelength, the number of propagating modes increases to two. This number increases further by the normalized width of the slits.

As can be seen in Fig. 2, there are many eigen-modes in the structure with non-zero attenuation constants. These modes cannot contribute to considerable power transmission for thick gratings. One type of these modes is the nearly pure evanescent modes that have small phase constants and thus their loci are close to the imaginary axis. In the calculated roots of Fig. 2, these evanescent modes are indicated using dashed-line circles. At a given wavelength, the number of such roots increases by the slit width a. This is shown in Fig. 2 for two different slit widths.

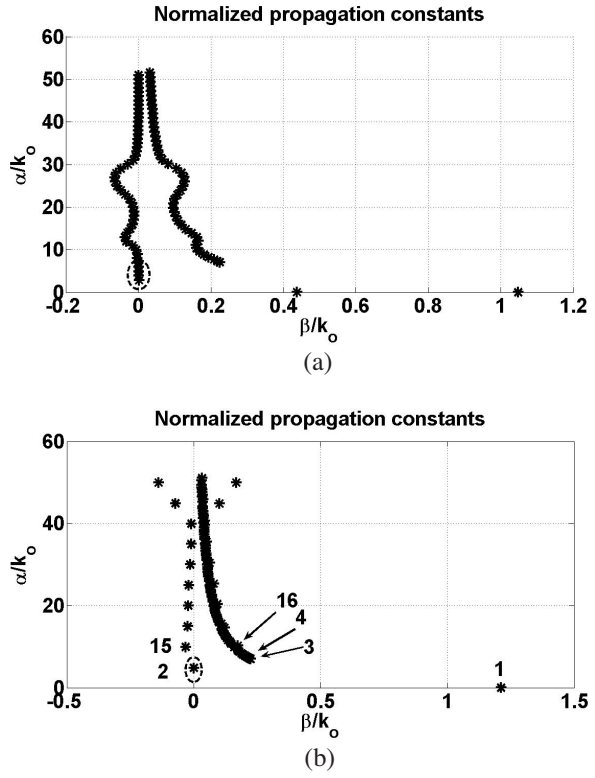

Figure 2. Calculated roots of the characteristic equation for two different slit widths at $\lambda_o = 1\,\mu$m for $d/\lambda_o = 0.96$ and $\varepsilon_r = -48.8 - j3.16$ for silver [19], (a) the slit width is $a/\lambda_o = 0.5$ (b) the slit width is $a/\lambda_o = 0.1$.

The evanescent roots with non-zero phase constants form another set of modes. In the metallic gratings, the non-zero imaginary part of the dielectric constant makes some of the roots, which otherwise were purely evanescent roots for a lossless structure, have a non-zero phase constant. These modes may have positive or negative phase constants.

As an example, for the parameters of Fig. 2(b), the normalized propagation constants along the y-axis in the metallic ($v_n = v'_n + jv''_n$) and air ($u_n = u'_n + ju''$) regions are demonstrated in Figs. 3(a) and (b), respectively.

The modes are enumerated according to their attenuation constants in the z-direction. They are illustrated in Fig. 2(b), where the modes with smaller attenuation are of the lower orders.

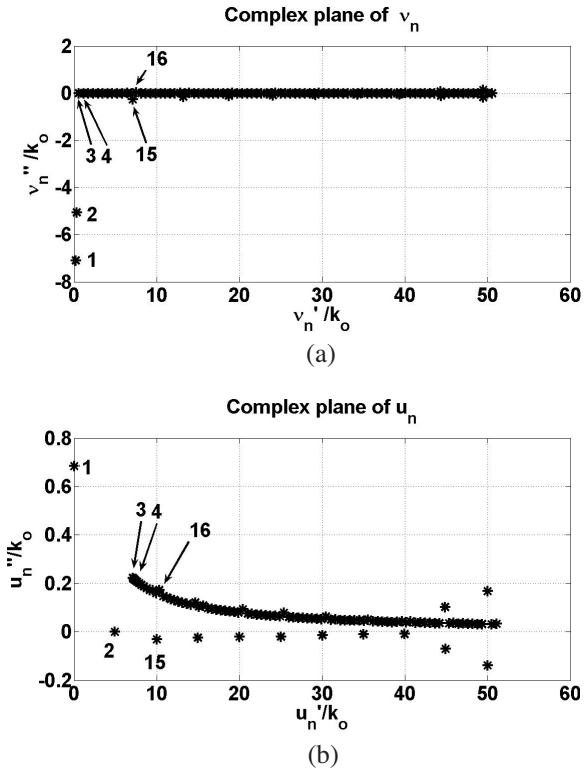

Figure 3. Normalized propagation constants along y-axis at $\lambda_o = 1\,\mu$m, $d/\lambda_o = 0.96$ and $a/\lambda_o = 0.1$, (a) in the metallic region (v_n), (b) in the air region (u_n).

Considering the propagation constants along the grating vector (the y-axis) in Fig. 3, we realize that for nearly pure evanescent modes e.g., mode 2 in Fig. 2(b) the propagation coefficient in the metallic region (v_n) has a large imaginary part, so these modes only slightly penetrate into the metal. But in the air region their propagation coefficient (u_n), is nearly real. This means that these modes have a standing wave nature in the slits. The H_x field distribution of this nearly pure evanescent root, i.e., mode 2 of Fig. 2(b), is demonstrated in Fig. 4(a).

For the evanescent modes with positive phase constants on the branch, like mode 3 and 4, we have $v_n''/v_n' \ll 1$ in the metallic region, so they form standing waves in the metal. In the air region, their attenuation in the y-direction is defined by the ratio u_n''/u_n'. Field

distribution of one mode of this kind, mode 3, is demonstrated in Fig. 4(b). For the evanescent modes with negative phase constants, such as mode 15, we have $u_n''/u_n' \ll 1$ which means that they are comprised of standing waves in the air region, and depending on their v_n''/v_n', they may be attenuated in the metallic region. For any of the modes with negative phase constant, there is a related mode with positive phase constant of equal attenuation constant. For instance, the field distributions of mode 15 and its related mode, that is mode 16, are illustrated in Figs. 4(c) and (d), respectively. These two modes are related to the transverse resonances in the slits; the periodic occurrence of such roots that is related to the ratio of a/λ_o proves this. For instance, the spacing of the left-hand-sided modes in Fig. 2(a) is smaller than the corresponding spacing in Fig. 2(b). This is because a/λ_o is larger in Fig. 2(a) than Fig. 2(b). The periodicity in k_z-loci is defined by $\lambda_o/2a$ which is a result of the periodicity of these roots around the real axis in the u_n plane, as Fig. 3(b) suggests.

4. TRANSMISSION ANALYSIS

Using the modes determined in the previous section, we apply the method of mode matching to evaluate the power transmission through the slit array. For this purpose, the Rayleigh expansions in the homogeneous regions I and III are matched to a linear combination of the obtained modes within region II. The coefficients of this linear combination and those of the Rayleigh expansions are determined by equaling the tangential field components at the interface of region I and II, as well as region II and III. Note that the modes computed in region II are not orthogonal [20], which results in full matrices in matching of tangential fields.

Using this method, we can obtain the transmission and the power loss in the metallic parts at $\lambda_o = 1\,\mu$m for $a/\lambda_o = 0.1$ and $h/\lambda_o = 0.15$. The dielectric constant of silver is $\varepsilon_r = -48.8 - j3.16$ at this wavelength [19]. Figs. 5(a) and (b) illustrate the computed transmission and normalized power loss as a function of the normalized period d/λ_o, respectively.

In this figure, we can recognize two transmission zeros that occur at the periods that are multiples of surface plasmon wavelengths. There are two maxima close to the transmission zeros. The maximum that occurs at $d/\lambda_o = 2$, is due to Wood's anomaly because d/λ_o assumes an integer number. The surface plasmon wavenumber is given

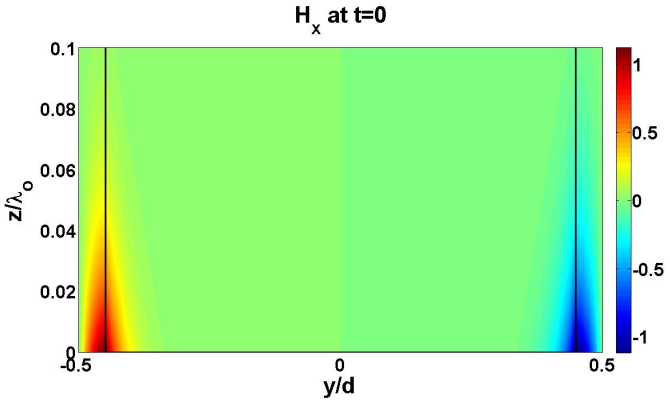
H_x at t=0
z/λ_o
y/d
0.1
0.08
0.06
0.04
0.02
0
-0.5
0
0.5
1
0.5
0
-0.5
-1

(a)

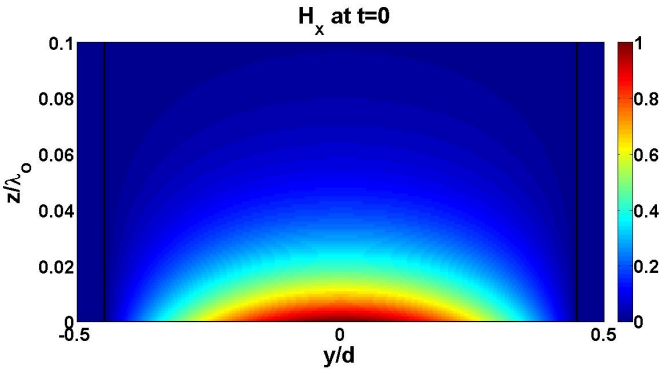
H_x at t=0
z/λ_o
y/d
0.1
0.08
0.06
0.04
0.02
0
-0.5
0
0.5
1
0.8
0.6
0.4
0.2
0

(b)

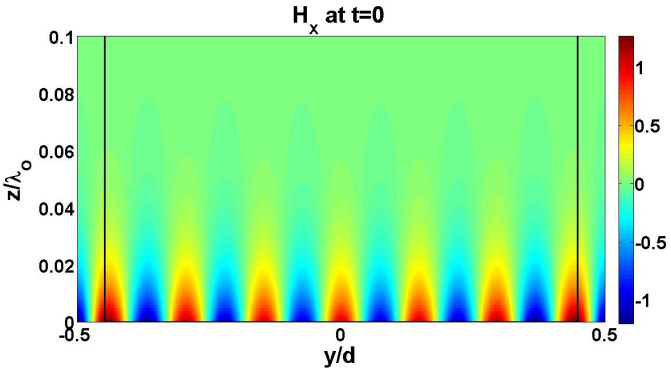
H_x at t=0
z/λ_o
y/d
0.1
0.08
0.06
0.04
0.02
0
-0.5
0
0.5
1
0.5
0
-0.5
-1

(c)

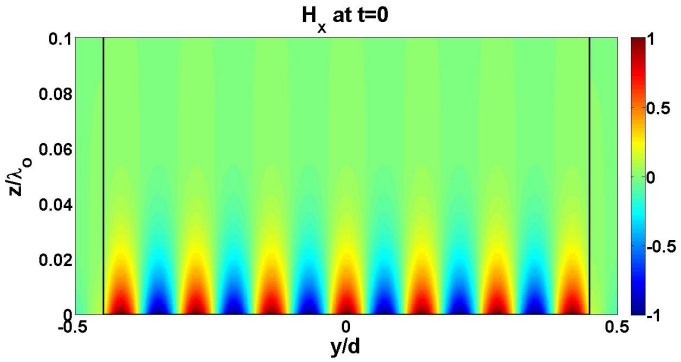

(d)

Figure 4. H_x field distributions for different modes at $\lambda_o = 1\,\mu$m, $d/\lambda_o = 0.96$ and $a/\lambda_o = 0.1$, (a) mode 2, the purely evanescent mode of the structure, (b) mode 3, first mode on the branch, (c) mode 15, the mode with negative phase constant, (d) mode 16, the related mode to mode 15.

by

$$k_{sp} = k_0\sqrt{\frac{\varepsilon_{rd}\varepsilon_{rm}}{\varepsilon_{rd}+\varepsilon_{rm}}} = \frac{2\pi}{\lambda_{sp}} \tag{8}$$

therefore, surface plasmons are expected at $d/\lambda_o = 0.99 \approx \lambda_{sp}/\lambda_o$, where there is the first transmission zero. At that point the amplitude of the propagating mode of the slit is very small while one of the evanescent modes is excited mostly. The loci of the roots of the characteristic equation and the calculated mode amplitudes at $d/\lambda_o = 0.99$ are demonstrated in Figs. 6(a) and (b), respectively.

In Fig. 6(a), the modes are enumerated in accordance with the value of their attenuation constants. For $d/\lambda_o = 0.99$ the third mode which has a resonant profile at the input boundary of the grating is mostly excited. When considering the power loss of different modes in the metallic parts of the grating it is understood that this mode absorbs the incident power mostly. At this period, different field components are visualized in Fig. 7.

Note that for all values of d/λ_o except for $d/\lambda_o = 0.99$ and its multiples, the excitation of the propagating mode is the most. For higher thicknesses of the grating, the excitation of the propagating mode can result in high transmission. This effect occurs for those thicknesses in which the grating can support Fabry-Perot-like

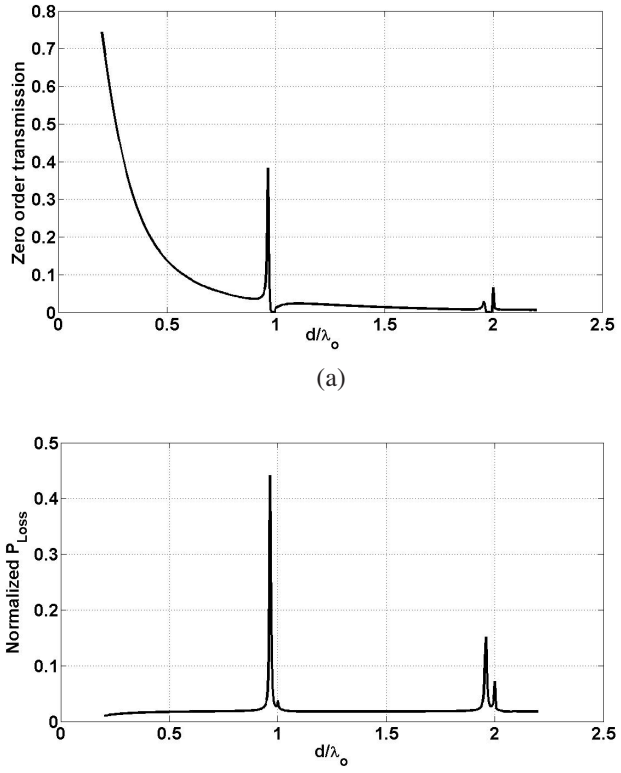

Figure 5. (a) Zero-order transmission at $\lambda_o = 1\,\mu$m. (b) Normalized power loss in the metallic region at $\lambda_o = 1\,\mu$m.

resonances in the slits. In thin gratings with respect to the wavelength, the Fabry-Perot condition, $h = n\lambda_o/2$, can not be met thus, there should be another mechanism responsible for high transmission. At $d/\lambda_o = 0.965$ with a normalized thickness of $h/\lambda_o = 0.15$ studied in Figs. 5(a) and (b), both the power loss in the metallic region and the transmission through the grating are large. Therefore, we believe that at $d/\lambda_o = 0.965$, the excitation of the surface plasmons is helping the transmission and couples the power to the propagating mode. As the two dielectrics above and below the grating are the same, i.e., air, both interfaces have the same surface plasmon wavelengths so the propagating mode couples the power to the surface plasmons of the output face which results in high transmission. In Figs. 8(a) and (b), the loci of the roots of the characteristic equation and the calculated

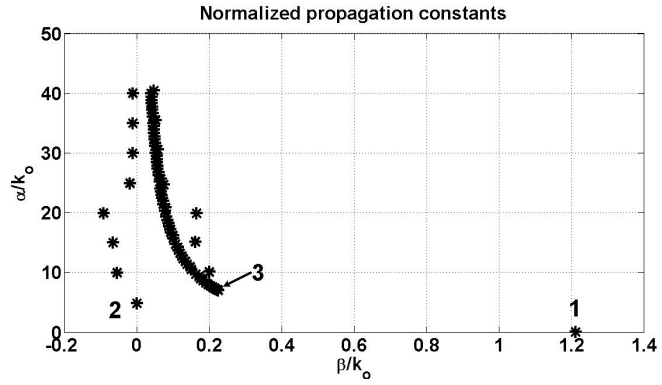

(a)

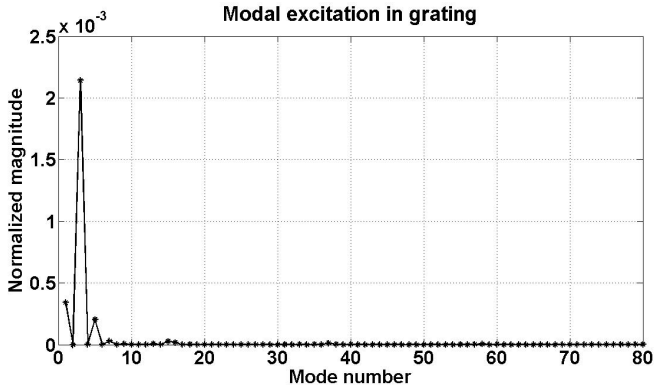

(b)

Figure 6. (a) Loci of the roots at the first transmission zero ($d/\lambda_o = 0.99 \approx \lambda_{sp}/\lambda_o$), (b) Mode amplitudes at the same period.

mode amplitudes at $d/\lambda_o = 0.965$ are demonstrated, respectively. Note that the excited amplitude of the third mode in comparison to the amplitude of the propagating mode is small but it is more than the amplitude of the third mode even at $d/\lambda_o = 0.99$.

In Figs. 9(a) and (b), the transmission efficiency and normalized power loss in the metallic parts are illustrated sweeping both the grating period and thickness. For comparison with the results in [18], we have illustrated the transmission efficiency, which is defined as the ratio of the total power integrated over one period at the output interface to the total power incident to the slit width a on the input interface.

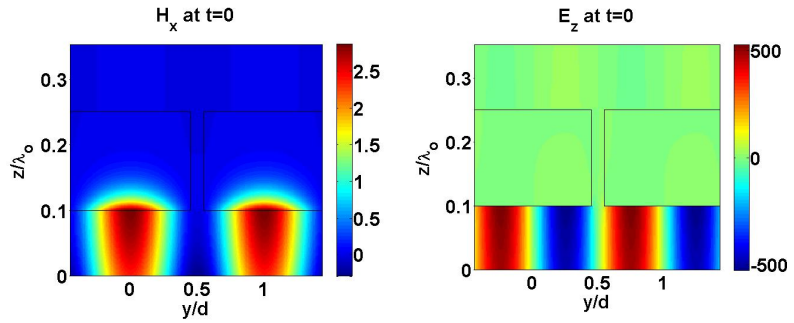

(a) (b)

Figure 7. Field distributions at a transmission zero ($d/\lambda_o = 0.99 \approx \lambda_{sp}/\lambda_o$), (a) H_x, (b) E_z.

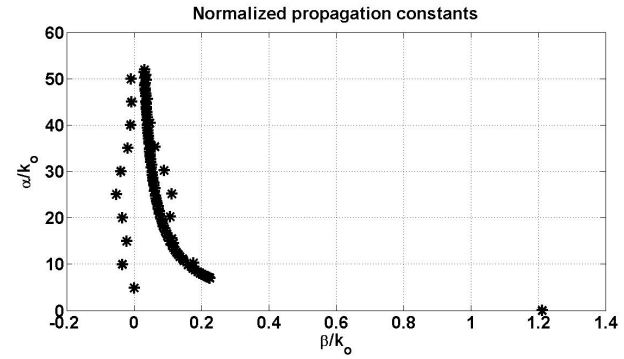

(a)

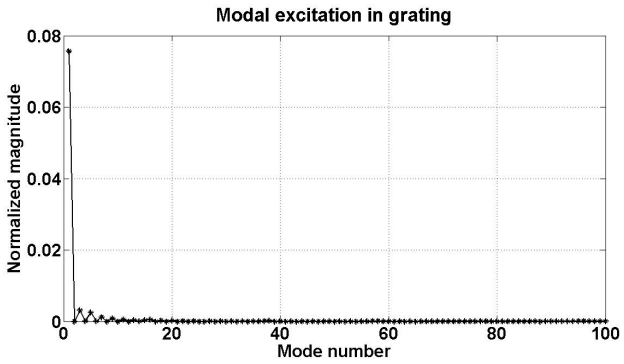

(b)

Figure 8. (a) Loci of the roots at the maximum of transmission ($d/\lambda_o = 0.965$), (b) Mode amplitudes at the same period.

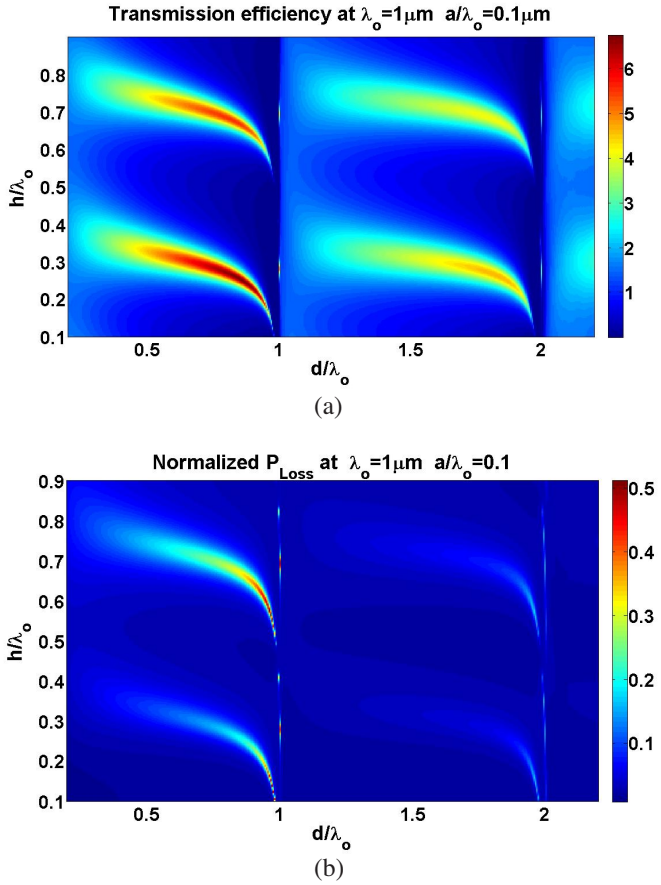

Figure 9. (a) Transmission efficiency at the wavelength $\lambda_o = 1\,\mu$m and $a/\lambda_o = 0.1$, (b) the normalized power loss in the metallic parts.

As the period decreases below the surface plasmon wavelength, the transmission changes gradually to the Fabry-Perot type known in thicker gratings. The power loss in the metallic parts decreases, too, which is in agreement with the gradual changing of the transmission mechanism. The reason is that the source of power dissipation in metallic parts which are the excitations of the surface waves is diminished. Using this exact modal method along with mode matching technique enables us to consider all types of phenomenon in the gratings, like Wood's anomaly that are illustrated in Fig. 9, which were not observed in a similar investigation through FDTD [18].

5. CONCLUSIONS

In this work, we examined different modes in metallic gratings, their characteristics, and the parameters effective on them. We also investigated the mechanisms responsible for the transmission in metallic gratings, the Fabry-Perot like resonances and the surface plasmon excitation. The high transmission around the surface palsmon wavelength is really dependant on surface plasmons and the two phenomena cooperate in increasing the transmission. As the period decreases, the transmission changes gradually to the Fabry-Perot type known in thicker gratings.

ACKNOWLEDGMENT

The authors wish to acknowledge the support of the Iran Telecommunication Research Center (ITRC). The authors also wish to acknowledge helpful discussions with our colleague, Mr. Nima Dabidian.

REFERENCES

1. Reather, H., *Surface Plasmons on Smooth and Rough Surfaces and on Gratings*, Springer-Verlag, Berlin, 1986.
2. Suyama, T., Y. Okuno, and T. Matsuda, "Plasmon resonance-absorption in a metal grating and its application for refractive-index measurement," *Journal of Electromagnetic Waves and Applications*, Vol. 20, No. 2, 159–168, 2006.
3. Lin, L., R. J. Blaikie, and R. J. Reeves, "Surface-plasmon enhanced optical transmission through planar metal films," *Journal of Electromagnetic Waves and Applications*, Vol. 19, No. 13, 1721–1728, 2005.
4. Kong, F. M., K. Li, B. I. Wu, et al., "Propagation properties of the SPP nano scale narrow metallic gap, channel, and hole geometries," *Progress In Electromagnetics Research*, PIER 76, 449–466, 2007.
5. Arnold, M. D., "An efficient solution for scattering by a perfectly conducting strip grating," *Journal of Electromagnetic Waves and Applications*, Vol. 20, No. 7, 891–900, 2006.
6. Kalhor, H. A. and M. R. Zunoubi, "Electromagnetic scattering and absorption by arrays of lossless/lossy metallic or dielectric strips," *Journal of Electromagnetic Waves and Applications*, Vol. 19, No. 4, 497–512, 2005.

7. Li, B., "Study on high gain circular waveguide array antenna with metamaterial structure," *Progress In Electromagnetics Research*, PIER 60, 207–219, 2006.
8. Hamid, A.-K., "Axially slotted antenna on a circular or elliptic cylinder coated with metamaterials," *Progress In Electromagnetics Research*, PIER 51, 329–341, 2005.
9. Bethe, H. A., "Theory of diffraction by small holes," *Phys. Rev.*, Vol. 66, 163–182, 1944.
10. Ebbesen, T. W., H. J. Lezec, H. F. Ghaemi, T. Thio, and P. A. Wolff, "Extraordinary optical transmission through subwavelength hole arrays," *Nature*, Vol. 391, 667–669, 1998.
11. Porto, J. A., F. J. Garcia-Vidal, and J. B. Pendry, "Transmission resonance on metallic gratings with very narrow slits," *Phys. Rev. Lett.*, Vol. 83, 02845–02849, 1999.
12. Collin, S., F. Pardo, R. Teissier, and J. L. Pelouard, "Horizontal and vertical surface resonances in transmission metallic gratings," *J. Opt. A: Pure Appl. Opt.*, Vol. 4, S154–S160, 2002.
13. Cao, Q. and P. Lalanne, "Negative role of surface plasmons in the transmission of metallic gratings with very narrow slits," *Phys. Rev. Lett.*, Vol. 88, 057403-1–057403-4, 2002.
14. Treacy, M. J., "Dynamical diffraction on explanation of the anomalous transmission of light through metallic gratings," *Phys. Rev. B*, Vol. 66, 195105-1–195105-11, 2002.
15. Lalanne, P., J. P. Hugonin, S. Astilean, M. Palamaru, and K. D. Moller, "One-mode model and Airy-like formulae for one-dimensional metallic gratings," *J. Opt. A: Pure Appl. Opt.*, Vol. 2, 48–51, 2000.
16. Garcia-Vidal, F. J. and L. Martin-Moreno, "Transmission and focusing of light in one-dimensional periodically nanostructured metals," *Phys. Rev. B*, Vol. 66, 155412-1–155412-10, 2002.
17. Xie, Y., A. R. Zakharian, J. V. Moloney, and M. Mansuripur, "Transmission of light through periodic arrays of sub-wavelength slits in metallic hosts," *Opt. Exp.*, Vol. 14, 6400–6413, 2006.
18. Xie, Y., A. R. Zakharian, J. V. Moloney, and M. Mansuripur, "Transmission of light through a periodic array of slits in a thick film," *Opt. Exp.*, Vol. 13, 4485–4491, 2005.
19. Palik, E. D., *Handbook of Optical Constants of Solids*, Academic Press, London, 1985.
20. Snyder, A. W. and J. D. Love, *Optical Waveguide Theory*, Chapman and Hall, London, 1983.